

1 **Motile bacteria leverage bioconvection for eco-physiological benefits in a natural** 2 **aquatic environment**

3 Francesco Di Nezio^{1,2*}, Samuele Roman^{1,3}, Antoine Buetti-Dinh¹, Oscar Sepúlveda
4 Steiner^{4,5}, Damien Bouffard⁴, Anupam Sengupta⁶ and Nicola Storelli^{1,2*}

5 ¹University of Applied Sciences and Arts of Southern Switzerland (SUPSI), Department of Environment,
6 Constructions and Design, Institute of Microbiology, Via Flora Ruchat-Roncati 15, 6850 Mendrisio,
7 Switzerland. ²University of Geneva, Department of Plant Sciences, Boulevard d'Yvoy 4, 1205 Geneva,
8 Switzerland. ³Alpine Biology Center Foundation, Via Mirasole 22A, 6500 Bellinzona, Switzerland. ⁴Swiss
9 Federal Institute of Aquatic Science and Technology (Eawag), Department of Surface Waters - Research
10 and Management, Seestrasse 79, 6047 Kastanienbaum, Switzerland. ⁵Civil & Environmental Engineering,
11 University of California – Davis, 3155 Ghausi Hall, Davis, CA 95616, USA. ⁶Physics of Living Matter,
12 Department of Physics and Materials Science, 162A Avenue de la Faïencerie, L-1511 Luxembourg City,
13 Luxembourg. *Email: francesco.dinezio@supsi.ch; nicola.storelli@supsi.ch

14 **Abstract**

16 Bioconvection, the active self-sustaining transport phenomenon triggered by the
17 accumulation of motile microbes under competing physico-chemical cues, has been long
18 studied, with recent reports suggesting its role in driving ecologically-relevant fluid flows.
19 Yet, how this collective behaviour impacts the ecophysiology of swimming microbes remains
20 unexplored. Here, through physicochemical profiles and physiological characterizations
21 analysis of the permanently stratified meromictic Lake Cadagno, we characterize the
22 community structure of a dense layer of anaerobic phototrophic sulfur bacteria, and report
23 that the associated physico-chemical conditions engender bioconvection when bulk of the
24 motile purple sulfur bacterium *Chromatium okenii* synchronize their movement against the
25 gravity direction. The combination of flow cytometry and fluorescent *in situ* hybridization
26 (FISH) techniques uncover the eco-physiological effects resulting from bioconvection, and
27 simultaneous measurements using dialysis bags and ¹⁴C radioisotope, allowed us to
28 quantify *in situ* the diurnal and nocturnal CO₂ fixation activity of the three co-existing species

29 in the bacterial layer. The results provide a direct measure of the cellular fitness, with
30 comparative transcriptomics data – of *C. okenii* populations present in regions of
31 bioconvection vis-à-vis populations in bioconvection-free regions – indicating the transcripts
32 potentially involved in the bioconvection process. This work provides direct evidence of the
33 impact of bioconvection on *C. okenii* metabolism, and highlights the functional role of
34 bioconvection in enhancing the metabolic advantage of *C. okenii* relative to other microbial
35 species inhabiting the microbial layer.

36

37

38 **Introduction**

39 Bioconvection is a well-known collective behavior observed in diverse groups of motile
40 microorganisms, from bacteria, to algae, to protists, which share a common upward-
41 swimming behavior and a density higher than water^{1–3}. The convective motion is triggered
42 when a large number of such microorganisms accumulates in a water body, leading to an
43 increase in local density and the subsequent formation of a density-unstable fluid ambient.
44 As a result, the denser mixture of water and microorganisms generates hydrodynamic
45 instabilities with the underlying water whereby the denser cell-rich layer comes down due
46 to the gravity force in the form of characteristic ‘plumes’. The bioconvection cycle is
47 sustained by the microorganisms carried away from the sub-surface layer being replaced
48 by others upswimming from below, generating a convective cycle^{4–6}.

49 Microbial bioconvection in natural aquatic settings is triggered when up-swimming cells
50 accumulate in competing gradients – physical or chemical – which get established due to
51 the local processes⁷. While the focus of earlier studies on bioconvection has been on
52 photo- and gyrotaxis^{7,8}, more recent works have indicated the possibility that microbes
53 could harness bioconvection for eco-physiological advantage, particularly in quiescent
54 aquatic environments, for instance in meromictic lakes. In general, however, the
55 physiological and ecological implications of microbial bioconvection still remain to be
56 clarified.

57 Meromictic lakes exhibit permanent density stratification and vertical gradients of light and
58 redox conditions. Their water column hosts several physiological groups of
59 microorganisms distributed along these vertical gradients, which act as specific ecological
60 niches. These characteristics make them an exemplary field-scale laboratory for studying
61 anaerobic microorganisms and their associated biogeochemical processes^{9–11}. In the
62 particular case of shallow chemocline (i.e. with depth scaling with the photic zone), light
63 penetration can promote large microbial blooms throughout the chemocline, with for

64 instance blue-green algae in its upper part and phototrophic sulfur bacteria in its lower
65 part^{12,13}. Lake Cadagno is an iconic example of crenogenic meromixis, a phenomenon
66 occurring when saline springs discharge dense water onto a freshwater lake depression,
67 setting up density stabilizing conditions¹⁴. As a result, the water column is permanently
68 stratified into an oxic, electrolyte-poor mixolimnion, a salt-rich, sulfidic monimolimnion and
69 an intervening chemocline at 10.0 – 12.0 m depth with reverse oxidoreductive gradients,
70 such as the disappearance of oxygen and the appearing of sulfide¹⁵.

71 One of the main features of Lake Cadagno is the diverse community of anoxygenic
72 phototrophic sulfur bacteria that develops in the chemocline proximity characterized by
73 opposite gradients of sulfide (S²⁻) and light irradiance^{16–20}. This community forms a dense
74 bacterial layer (BL) and is composed of purple sulfur bacteria (PSB) and green sulfur
75 bacteria (GSB), a number of which have been successfully isolated and cultivated in the
76 laboratory^{21–24}. At the present day, PSB strains *Chromatium okenii* LaCa and *Thiodictyon*
77 *synthopicum* Cad16^T, and GSB *Chlorobium phaeobacteroides* 1VII D7, previously
78 isolated from Lake Cadagno and grown as pure cultures in the laboratory, are the
79 dominant phototrophic sulfur bacteria species in the BL. PSB and GSB play a major role in
80 the biogeochemical cycles of carbon²⁵, sulfur²⁶ and nitrogen²⁷. In particular, inorganic
81 carbon fixation has also been observed in the absence of light, under microoxic conditions,
82 especially in PSB^{28,29}.

83 Bioconvection can have important ramifications for microbes in natural settings, including
84 molecular transport over large environmental scales, physico-chemical ecology and spatio-
85 temporal distribution of microbes in aquatic ecosystems. Recently, by combining field and
86 laboratory studies with numerical modeling, Sommer *et al.*³⁰ demonstrated that the motile
87 PSB *Chromatium okenii* is able to trigger mixing through bioconvection, resulting from the
88 concerted movement of large portions of its population. Lake Cadagno was the first
89 example of bioconvection witnessed in a natural freshwater environment³⁰, so far limited to

90 a few observations in marine ecosystems or laboratory settings^{31–35}. However, the study
91 by Sommer *et al.* focused on the physical demonstration of the phenomenon without
92 exploring its consequences on microenvironmental conditions, microbial community, or
93 biogeochemical implications on the lake ecosystem.

94 Regular monitoring of Lake Cadagno water column has shown the occurrence of
95 bioconvection between June and late August^{30,36,37}. In this study, we compare physico-
96 chemical profiles and physiological characterizations at two different times of the summer
97 season, July and September 2020, when we observed the presence and absence of
98 bioconvection, respectively, to elucidate its eco-physiological effects on the BL microbial
99 community. Additionally, we carried out transcriptomics analyses of PSB *C. okenii*, the
100 actor of bioconvection, with the goal of identifying key genes involved in this process or,
101 more generally, in its seasonal behavior. Our results imply that bioconvection may provide
102 *C. okenii* with an ecological advantage over the coexisting phototrophic sulfur bacteria.

103 **Methods**

104 **Study site and sampling**

105 Lake Cadagno is located in the Piora Valley (46°33'N, 8°43'E) in the southern Swiss Alps.
106 The sampling was conducted on 16 July and 17 September 2020 using a pump-CTD
107 system (CTD115M, Sea & Sun Technology, Germany), as described in Di Nezio *et al.*³⁸.
108 For the physico-chemical characterization of the water column, *in situ* high vertical
109 resolution data (sampling at 16 Hz) were obtained during a first continuous downcast of
110 the CTD system from the lake surface down to ~18.0 m depth. During a second downcast,
111 after 30 min and in a different area, discrete water samples were collected from a total of 6
112 depths (between 12.0 m and 18.0 m) for bio-chemical analyses and from the top of the BL
113 for incubation experiments (see 'Radioisotope incubation and uptake analysis' section).
114 Profiles were recorded at sunrise on 16 July and 17 September 2020 at 05:15 h and 06:30
115 h, respectively. CTD profiles for determination of light regimes were measured at daytime
116 (17:00 h) on both days. Atmospheric radiation data at 10 min resolution for both sampling
117 campaigns were retrieved from a meteorological station (istSOS;
118 <https://hydromet.supsi.ch/>) close to the lake shore.
119 Water samples for microbiological (FISH and flow cytometry) and chemical (S²⁻, SO₄²⁻ and
120 CaCO₃) analyses were stored in 50 ml falcon tubes and processed within the following
121 hour, as described in Di Nezio *et al.*³⁸.

122

123 **Cell growth**

124 Phototrophic sulfur bacteria were grown in Pfennig's medium I³⁹ and cultivated in
125 laboratory under a light/dark photoperiod of 16/8 h with a light intensity of 38.9 $\mu\text{mol m}^{-2} \text{s}^{-1}$
126 PPF (photosynthetic photon flux density) within the photosynthetically active radiation
127 (PAR) range, measured with a portable LI-180 Spectrometer (LI-COR Biosciences,
128 Lincoln, NE), as in Di Nezio *et al.*³⁸.

129

130 **Bacterial layer microbial community analysis**

131 To describe the composition of the BL microbial community, cell counting was performed
132 through flow-cytometry (FCM), as described in Danza *et al.*²⁶. Bacterial populations were
133 distinguished by applying gates on cell size (forward scatter, FSC) of 0.1 - 1.0 μm for GSB,
134 2.0 - 4.0 μm for small-celled PSB and 4.0 - 10.0 μm for *C. okenii* (Fig. S1). Simultaneously,
135 fluorescent *in situ* hybridization (FISH) analyses were carried out on bacterial layer (BL,
136 zone with a turbidity > 10 FTU) water samples, as previously described in Decristophoris
137 *et al.*¹⁷ (Tab. S1), spotting 2 μl of fixed sample on gelatin coated slides (0.1% gelatin,
138 0.01% $\text{KCr}(\text{SO}_4)_2$) and observing them by epifluorescence microscopy using filter sets F31
139 (AHF Analysentechnik, Tübingen, Germany; D360/40, 400DCLP, D460/50 for DAPI) and
140 F41 (AHF Analysentechnik, HQ535/50, Q565LP, HQ610/75 for Cy3) at 100X
141 magnification.

142

143 **Radioisotope incubation and uptake analysis**

144 To test the photosynthetic efficiency of pure bacterial laboratory cultures, cells were grown
145 up to concentrations of 10^6 cells ml^{-1} (mid exponential phase), sealed in 50-cm-long
146 dialysis bags (inflated diameter of 62.8 mm; Karl Roth GmbH Co. KG, Germany), whose
147 membrane allows for diffusive transport of small molecules (< 20 kDa); thus, preventing
148 contamination of the incubated samples from the surrounding environment.

149 The dialysis bags were acclimatized to the chemocline conditions of Lake Cadagno for a
150 period of 4 weeks (from 15 June to 16 July 2020 and from 21 August to 17 September
151 2020) before the experiments, at varying depths between 12.20 – 12.40 m and 13.12 –
152 12.94 m in July and September, respectively.

153 To measure the amount of light reaching the incubation depth, the dialysis bags supporting
154 frame was equipped with HOBO UA-002–64 Pendant passive data loggers (Onset
155 Computer Corporation, MA), one at the top and one at the bottom of the structure,
156 measuring relative light (Lux; 180–1,200 nm) at 60 min intervals during the 4-weeks
157 acclimatization periods, as well as over the course of the 24 h ¹⁴C incubations (16-17 July
158 and 17-18 September 2020). Average daylight intensity values for June - July and August -
159 September recorded at the top and bottom of the dialysis support frame are shown in Fig.
160 S2.

161 The ¹⁴C-radioisotope uptake experiment was carried out on 16 July and 17 September
162 2020. The ¹⁴CO₂ assimilation of every selected microorganism, and a lake water sample
163 collected at the top of the BL, were quantified in sealed glass bottles after a day and night
164 incubation, both in July (at 12.28 m and 12.35 m depth) and September (at 12.63 m and
165 12.83 m depth).

166 The dissolved inorganic carbon concentration needed for the calculation⁴⁰ was determined
167 using the CaCO₃ Merck Spectroquant kit (No. 1.01758.0001) and the Merck Spectroquant
168 Pharo 100 spectrophotometer (Merck, Schaffhausen, Switzerland).

169

170 **Light and energy requirements calculations**

171 HOBO light and carbon assimilation data were used to calculate the quantum requirement
172 for the CO₂ fixation as the ratio between moles of photons absorbed and moles of ¹⁴CO₂
173 fixed by the BL and the dialysis bags pure cultures. Moles were correlated to the surface
174 area (m²) of the glass vials used for the ¹⁴C-incubation to calculate how many moles of
175 photons reached the surface of the vials over the entire light period⁴¹.

176

177 **RNA extraction, sequencing and analysis**

178 Samples for transcriptomic analysis were filtered (Isopore 0.22 mm PC Membrane, diam
179 25 mm) using a vacuum pump (Vacuumbrand, Wertheim, Germany) connected to a
180 filtration ramp (Pall, Basel, Switzerland) until the filter was completely clogged. Filters were
181 then immediately covered with RNAlater (QIAGEN, Hombrechtikon, Switzerland) for five
182 minutes and stored at -20°C.

183 RNA was extracted with the RNeasy Plus Universal Mini kit (QIAGEN) following the
184 'Purification of total RNA Using the RNeasy Plus Universal mini kit' protocol for the
185 TissueLyser II, using the complete filter as starting material and a mixture of glass beads
186 of different sizes (0,1 mm, 0,5 mm and 1 mm).

187 DNase treatment was performed using TURBO DNA-free kit (Invitrogen) following the
188 manufacturer's routine protocol. RNA was quantified fluorometrically at 260/290 nm and
189 260/230 nm using NanoDrop and the Qubit RNA HS Assay Kit (Invitrogen).

190 Complementary DNA, PCR and Barcoding of the specimens were performed using the
191 Nanopore SQK-PCB109 kit, according to the accompanying protocol.

192 For the Oxford Nanopore Technologies (ONT) library preparation, 50-100 fmol in 11 ml of
193 reverse transcribed DNA was used and sequencing performed with an ONT R9.4 flow cell,
194 following the manufacturer's instructions.

195 Basecalling and barcoding were performed using the 'accurate' option with ONT Guppy
196 software (version 5.0.7), using the command line procedure with the configuration file
197 'dna_r9.4.1_450bps_hac.cfg'. RNA quality assessment and postprocessing was performed
198 with ONT Pychopper (v2), followed by running the ONT long-reads pipeline for differential
199 gene expression (DGE) analysis⁴². The bioinformatics workflow employed Snakemake⁴³ to
200 run different steps including the following tools: minimap2, salmon, edgeR, DEXSeq and
201 stageR with options (minimap index opts: ""; minimap2 opts: ""; maximum secondary: 100;
202 secondary score ratio: 1.0; salmon libtype: "U"; min samps gene expr: 3; min samps
203 feature expr: 1; min gene expr: 10; min feature expr: 3). NCBI COG

204 (<https://www.ncbi.nlm.nih.gov/research/cog-project/>) was used to classify the predicted
205 genes into COG-categories.

206

207 **Statistical analysis**

208 Data are shown as mean \pm SD. All the measurements were taken from distinct samples.

209 Statistical significance was assessed by two-way ANOVA for parametrical data, as

210 indicated; Šidák test was used as a post-hoc test. For multiple comparisons, multiplicity

211 adjusted p-values are indicated in the corresponding figures. Statistical analyses

212 comprising calculation of degrees of freedom were done using GraphPad Prism 9.5.1.

213

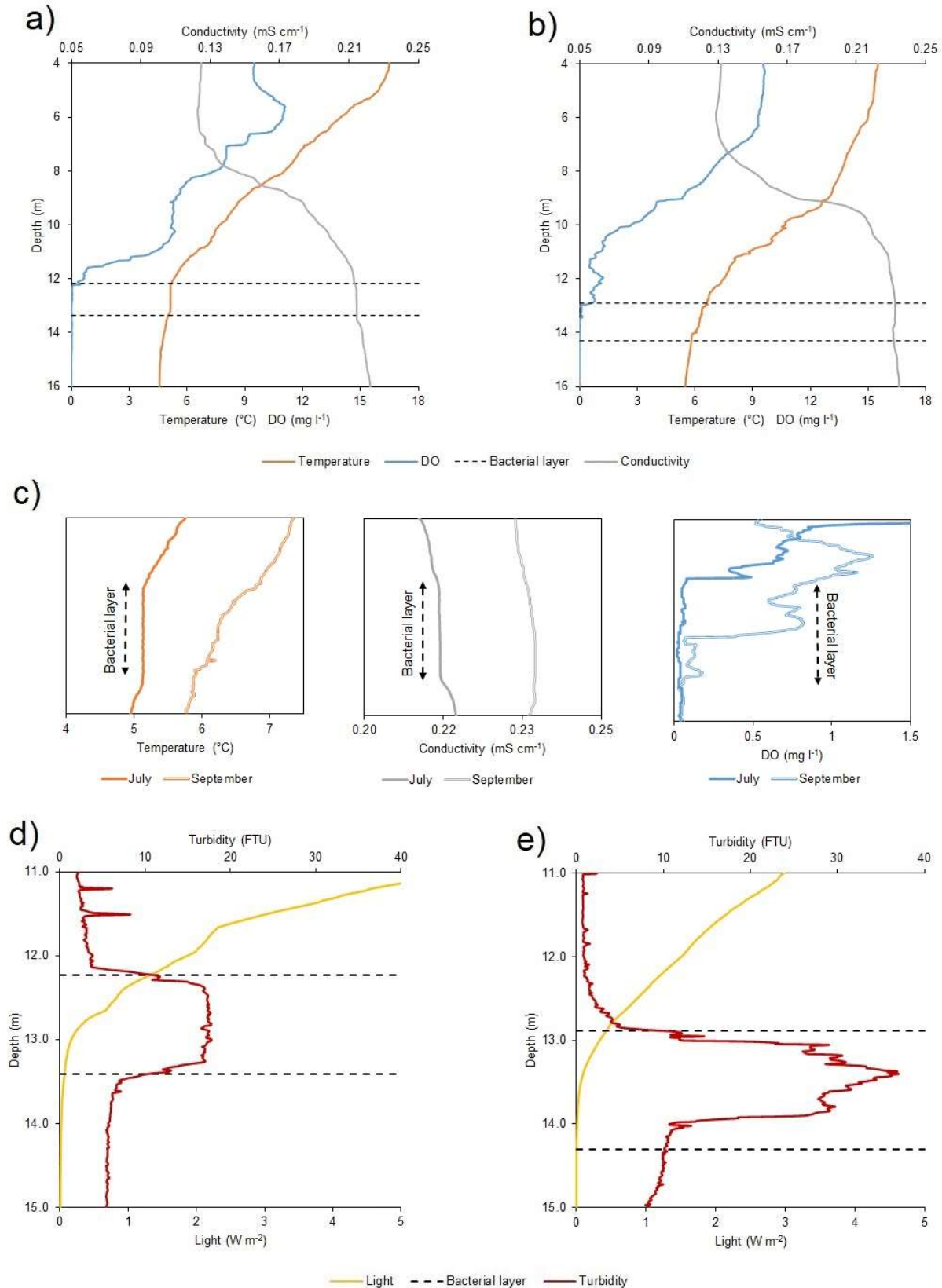
214

215 **Results**

216 **Monitoring of the water column**

217 The physico-chemical profile of Lake Cadagno remained substantially unvaried between
218 July and September 2020 (Fig. 1). Parameters measured with the CTD such as dissolved
219 oxygen (DO), light, turbidity, temperature, and conductivity showed little difference
220 between the two periods throughout the water column, except for the location of the
221 turbidity peak and consequently the light intensity reaching the BL. On 16 July 2020, the
222 1.2 m wide BL lied between 12.18 - 13.36 m depth, with a maximum turbidity value of 17.7
223 FTU at a depth of about 12.70 m (Fig. 1d), while on 17 September 2020, it was nearly 20
224 cm wider (1.4 m) and about 70 cm deeper (12.89 – 14.30 m depth) with a maximum
225 turbidity peak of 36.9 FTU almost a meter deeper than in July, at 13.40 m (Fig. 1e). Such
226 difference in depth resulted in a disparate light profile with an intensity reaching the BL top
227 of 0.44 W m^{-2} in September, twice lower than in July with 0.88 W m^{-2} (Fig. 1d, e).
228 Dissolved oxygen showed an irregular profile on 16 July, with the presence of a production
229 peak around 5 m and a minor one around 11 m depth (Fig. 1a), suggesting photosynthetic
230 activity. In September, on the other hand, the profile decreased more linearly without any
231 peak (Fig. 1b). It is relevant to note how in July, and not in September, temperature,
232 conductivity and oxygen at the peak of turbidity showed a homogeneous profile, indicating
233 the presence of a mixed layer due to bioconvection (Fig. 1c). These time points were
234 selected based on the long-term data sets available from the Lake Cadagno monitoring.

235



236

237 **Fig. 1 Physicochemical profiles of Lake Cadagno water column.** CTD profiles of oxygen (mg l⁻¹), temperature (°C),

238 and temperature-corrected (20°C) conductivity (mS cm⁻¹) in **a)** July and **b)** September. **c)** Temperature (*left*),

239 temperature-corrected conductivity (*central*) and DO (*right*) microstructure profiles for the BL and adjacent regions

240 observed on the two different moments of the year 2020. Different light irradiance ($W m^{-2}$) and turbidity (FTU) values
241 within the BL observed between **d**) July and **e**) September. Black dashed lines indicate the BL position on both sampling
242 days (16 July and 17 September 2020).

243

244 **Differences in light availability**

245 Data collected with the CTD revealed a difference in the duration and intensity of light in
246 the BL region between July and September. The nearby meteorological station showed an
247 average photoperiod in July of around 16.0 h (05:15 - 21:20) while in September it reduced
248 to about 12.5 h (06:40 – 19:20 h). This resulted in a PAR portion of the average incident
249 radiation below the lake subsurface (1 cm depth) of $100.85 W m^{-2} day^{-1}$ on 16 July and
250 $43.62 W m^{-2} day^{-1}$ on 17 September and, consequently, light radiation reaching the top of
251 the BL was higher in July (Tab. 2). Moreover, in September the larger values of observed
252 turbidity (Fig. 1e) determined a greater degree of light attenuation across the BL. As a
253 consequence, the shading effect exerted by the turbidity peak ultimately caused no light to
254 reach the lower part of the BL (Tab. 2).

255

256 **Table 1** Lake Cadagno and BL light regimes ($W m^{-2} day^{-1}$) during the two sampling days.

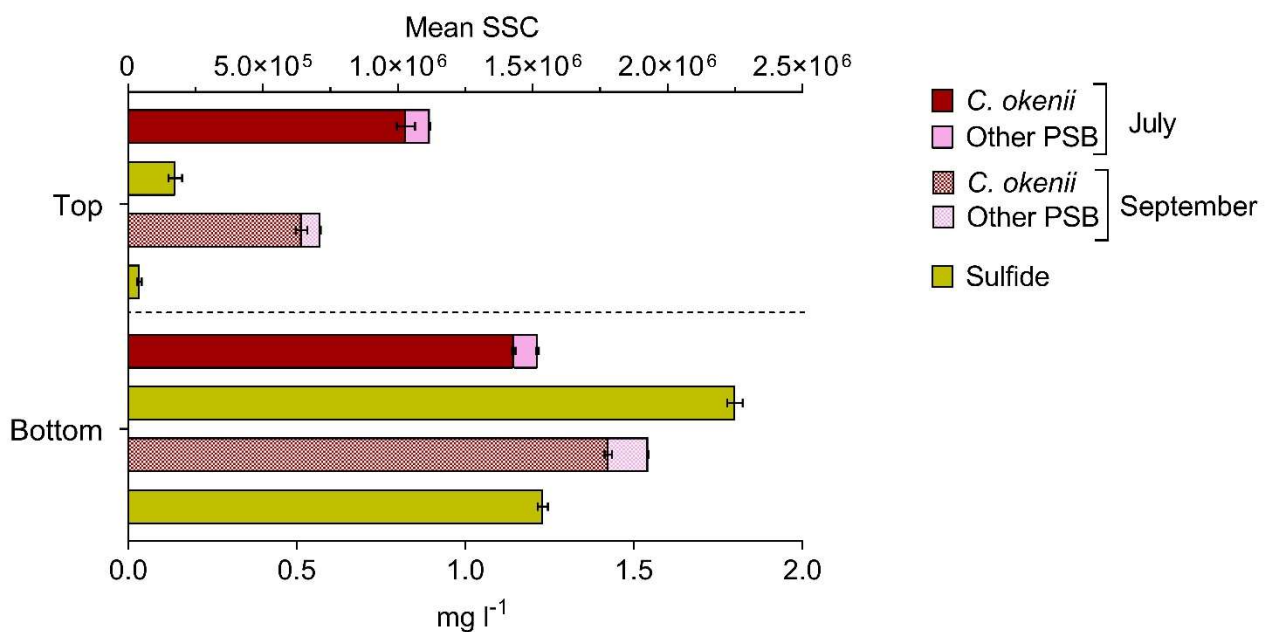
Date	Light period (h)	Lake subsurface	Top BL	Bottom BL
16.07.20	16.0	100.85	1.44	0.06
17.09.20	12.5	43.62	0.44	0.00

257

258 **Sulfide concentrations across the BL**

259 On 16 July, S^{2-} concentration measured at sunrise, before the light reached the BL, was
260 around $0.14 mg l^{-1}$ at the top of the BL and $1.88 mg l^{-1}$ at the bottom, while on 17
261 September, at the same moment of the day, sulfide concentration at the top was zero
262 (under the detection limit of $0.03 mg l^{-1}$) and $1.23 mg l^{-1}$ at the bottom (Fig. 2; yellow bars).

263 The more homogeneous S^{2-} gradient observed at sunrise in July is also visible when
264 expressing sulfide concentration across the BL as percentage of the concentration at the
265 bottom (Fig. S3).
266 Interesting to note are the different values of sideward scatter signal (SSC) measured via
267 Flow Cytometry (FCM) (Fig. 2; red and pink bars), which indicates cellular complexity that,
268 for PSB, largely depends on the presence of intracellular sulfur globules⁴⁴. Indeed, in
269 September a decrease in the amount of cell complexity at the top BL was observed in
270 areas gated for *C. okenii* and small-cell PSB in the FCM scatter plots (Fig. S1b). These
271 findings together show that, in proximity of photic zone at the top BL, as sulfide
272 concentration reduces, *C. okenii* and all PSB in general resort to the oxidation of sulfur
273 globules, instead of S^{2-} , for their photosynthetic activity.



274
275 **Fig. 1** Flow cytometry mean sideward scatter (SSC) of *C. okenii* and small-celled PSB and corresponding sulfide
276 concentrations in the upper and lower part of the bacterial layer on 16 July and 17 September 2020. Error bars represent
277 standard deviation ($n = 3$).

278

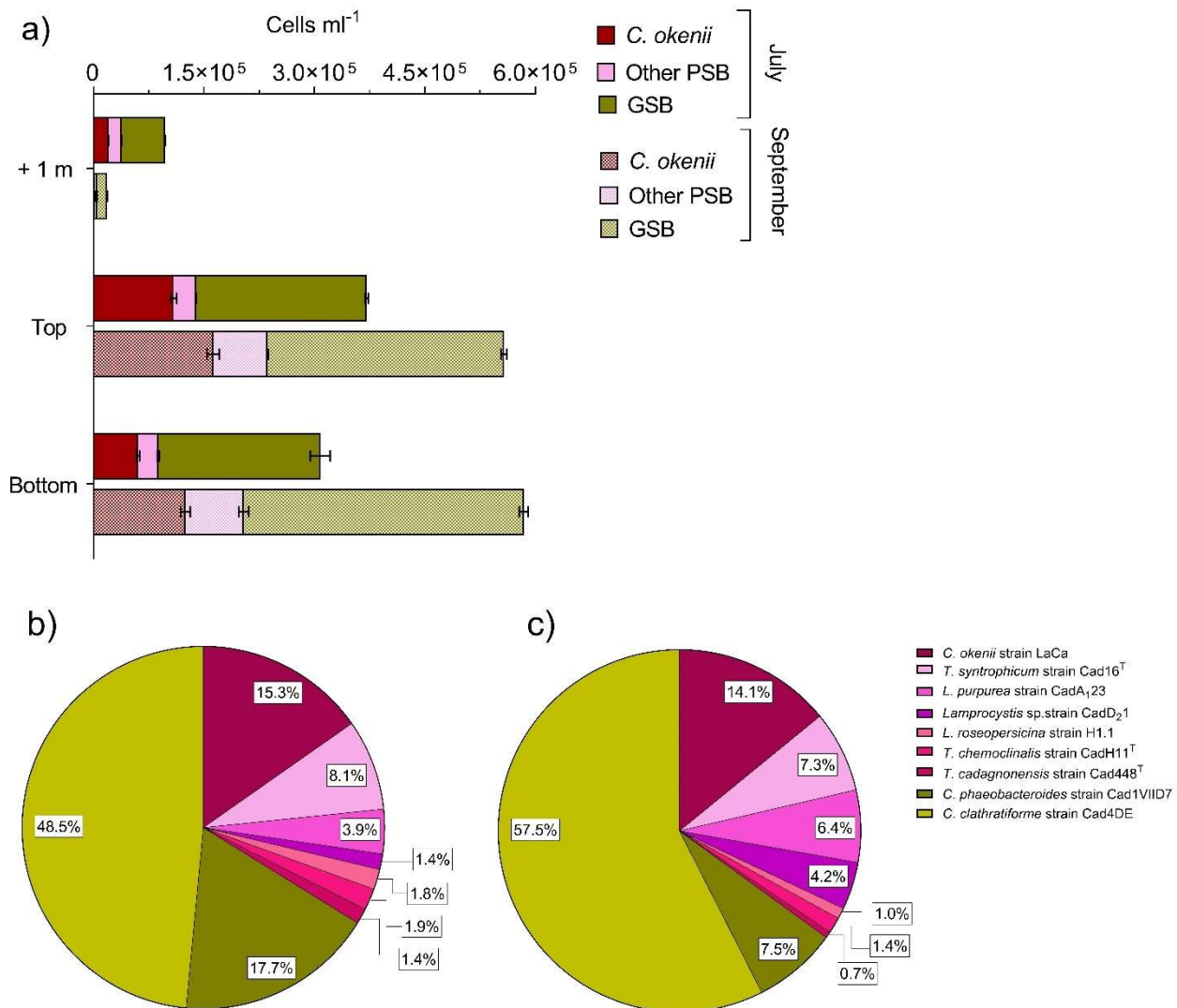
279 Differences in the BL community

280 FCM analysis of lake water samples showed high concentrations of photosynthetic
281 microorganisms, within the turbidity peak, in the BL (Fig. 3a).

282 In both periods analysed, concentration of large-celled *C. okenii* (approx. length 6 - 8 μm)
283 reached its maximum at the top of the BL, when the turbidity value exceeded 10 FTU,
284 where FCM red fluorescence signal revealed values of $1.09 \pm 0.03 \times 10^5$ cells ml^{-1} in July
285 and $1.63 \pm 0.08 \times 10^5$ cells ml^{-1} in September. The relative abundance of *C. okenii* then
286 decreased towards the lower part of the BL with cell concentrations down to $0.61 \pm 0.02 \times$
287 10^5 and $1.25 \pm 0.06 \times 10^5$ cells ml^{-1} in July and September, respectively (Fig. S1b, c; Fig.
288 3a).

289 Interestingly, in July during bioconvection, small-celled PSB and GSB were more abundant
290 one meter above the BL, outside the optimal anaerobic zone (5% and 16% of the total
291 counts at the top BL), while in September without bioconvection their numbers above the
292 BL were much lower, accounting for about 1% and 3% of the total cells at the top of the
293 BL, respectively.

294 Looking in more detail at the species-level composition of the top BL community, large-
295 celled PSB *C. okenii* and all GSB showed a slight decrease in September both about
296 1.2%, while small-celled PSB had a small increase of 2.4% (Fig. 3). Such increase in PSB
297 abundance, already revealed by FCM counts, was mainly due to PSB *Lamprocystis* sp.,
298 strains CadA₁₂₃ and CadD₂₁ which doubled, from 3.9 to 6.4 %, and quadrupled their
299 counts from 1.4 to 4.2 %, respectively. Among GSB, *Chlorobium clathratiforme* abundance
300 increased by about 9.0%, with a concomitant drop of *C. phaeobacteroides* cell number of
301 10.2% in September (Fig. 3c).



302

303

304

305

306

307

308

309 Seasonal differences in cell physiology

310

311

312

313

314

Fig. 2 a) Different abundances of anoxygenic phototrophic sulfur bacteria 1 m above, at the top and bottom of the BL between 16 July 2020 (full color) and 17 September 2020 (speckled color). Cell numbers ($\times 10^5 \text{ ml}^{-1}$) of all phototrophic sulfur bacteria in the BL obtained by FISH with probes S453F, S453A, S453E, S453H, S453D, S448, CHLP and CHLC at the top of Lake Cadagno BL on **b)** 16 July 2020 and **c)** 17 September 2020. Error bars represent standard deviation ($n = 3$).

To investigate the effect of seasonality on the physiology, C-fixation activity, both in presence or absence of light, was measured for the top BL and for single pure cultures of PSB *C. okenii* LaCa and *T. syntrophicum*, Cad16^T and GSB *C. phaeobacteroides* 1VII D7 incubated in dialysis bags at the corresponding depth of the BL. All samples were added with ¹⁴CO₂ and incubated for the whole 16 and 12.5 h light periods, and overnight for the

315 remaining hours, in July and September, respectively, at the corresponding top BL depths
 316 (12 and 13 m; Fig. 1d, e). HOBO loggers attached to the structure holding the dialysis
 317 bags (top and bottom) confirmed that the ^{14}C incubated samples were effectively exposed
 318 to the correct light intensity over the course of the experiment (Fig. S2).
 319 On 16 July 2020, the total assimilated $^{14}\text{CO}_2$ measured from the BL wild population after
 320 the diurnal incubation was more than four times higher the daily inorganic carbon fixation
 321 rate observed on 17 September 2020 (Fig. 4a; Tab. 2).
 322 Among the dialysis bags cultures incubated during daytime on 16 July, the highest $^{14}\text{CO}_2$
 323 fixation activity was measured in the large-celled *C. okenii* LaCa (Fig. 4b; Tab. 2). Diurnal
 324 assimilation of *T. syntrophicum* Cad16^T and *C. phaeobacteroides* 1VII D7 were one and
 325 three orders of magnitude lower, respectively (Fig. 4c, d; Tab. 2). In September, a 5-fold
 326 decrease in *C. okenii* daytime carbon fixation rate was observed, accompanied by a
 327 marked increase in the assimilation activity of both *T. syntrophicum*, which became the
 328 major CO_2 assimilator in September, and *C. phaeobacteroides* (Fig. 4c, d; Tab. 2).

329

330 **Table 2** July and September $^{14}\text{CO}_2$ mean assimilation rates (\pm SD) of the BL microbial community and dialysis bags
 331 incubated cultures. Values are reported in ^{14}C amol cell⁻¹ h⁻¹.

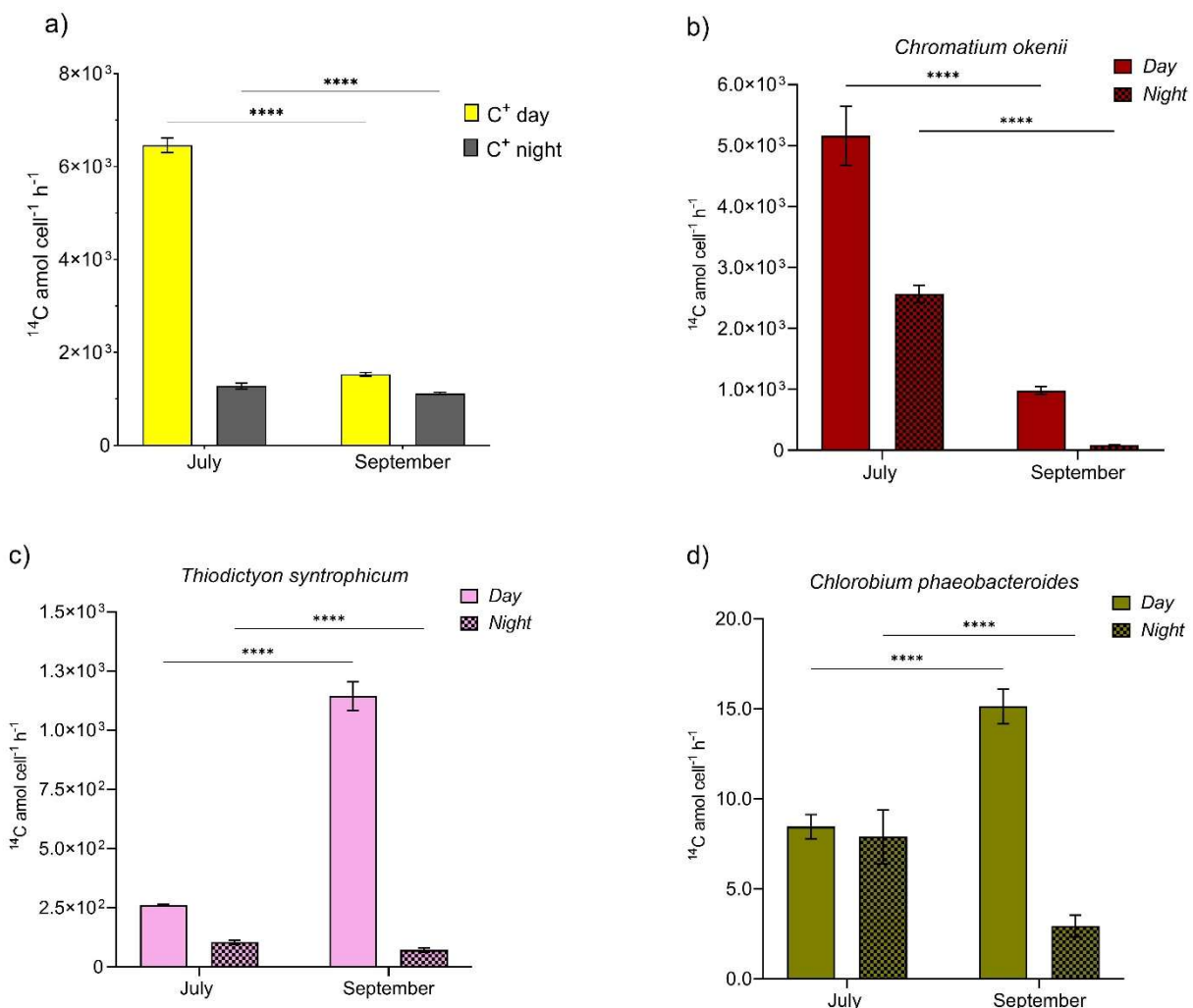
	July		September	
	Day	Night	Day	Night
Bacterial layer	6458 \pm 159.3	1278 \pm 62.6	1530 \pm 43.3	1118 \pm 27.0
<i>C. okenii</i>	5160 \pm 481.9	2565 \pm 140.6	981 \pm 63.2	87 \pm 6.0
<i>T. syntrophicum</i>	261 \pm 4.2	104 \pm 8.8	1144 \pm 60.1	71 \pm 8.0
<i>C. phaeobacteroides</i>	8.5 \pm 0.7	7.8 \pm 1.5	15 \pm 1.0	3.0 \pm 0.6

332

333

334 During the night, without any light irradiation, the total inorganic carbon assimilation of the
 335 BL decreased slightly from July to September (Fig. 4a; Tab. 2). Night *C. okenii*'s carbon
 336 fixation in July was still the highest among the three species, two to three orders of

337 magnitude higher than the values measured for *T. syntrophicum* Cad16^T and *C.*
338 *phaeobacteroides* 1VII D7, respectively (Fig. 4c, d; Tab. 2). Overall, dark CO₂ assimilation
339 of each single pure culture was higher in July than in September.
340 Microbial CO₂ fixation activity in the chemocline of Lake Cadagno was higher in daytime,
341 particularly in July when diurnal carbon assimilation of the BL microbial community was
342 more than double the night one (Fig. 4a). As for pure cultures, it is worth noticing the
343 strong activity of *C. okenii* during both day and night in July, which markedly decreases in
344 September by 81% and 94.3% day and night, respectively.



345
346 **Fig. 3 Primary production within the BL.** a) C-fixation activity of the top BL microbial community in July (left) and
347 September (right), expressed as total ¹⁴CO₂ assimilation rate (¹⁴C amol cell⁻¹ h⁻¹). b), c), d) ¹⁴CO₂ uptake by individual
348 pure cultures inside dialysis bags incubated during day (full color bars) and night (dotted color bars) at 12 (July) and 13

349 (September) m depth. Error bars represent standard deviation ($n = 3$). Error bars represent standard deviation ($n = 3$).
350 Two-way ANOVA followed by Šidák post hoc comparisons. (****) indicates adjusted P values < 0.0001 .

351

352 **Differences in the transcriptome of *C. okenii*.**

353 To assess the potential eco-physiological effect of bioconvection on the metabolic activity
354 of its main actor *C. okenii* LaCa, transcriptomic analysis was compared from both dialysis
355 bags cultures of 16 July and 17 September. Transcribed after-night, sunrise-isolated
356 genes from July were compared with those from September, as well as those expressed
357 after-day, sunset, also from July with those from September. After the day, 41 genes
358 resulted upregulated in September, and no one in July, while after night, 45 genes were
359 more expressed in September and 1 in July (Tab. S1, S2).

360 Of all the 86 genes upregulated from July to September, only in 4 cases it was possible to
361 associate the geneID with a functional category described in COG. The identified
362 categories were (i) signal transduction mechanisms, (ii) cell cycle control, cell division and
363 chromosome partitioning, (iii) translation, ribosomal structure and biogenesis, (iv) lipid
364 transport and metabolism and (v) energy production and conversion.

365

366 **Discussion**

367 This study provided for the first time clear indications of positive eco-physiological
368 implications of bioconvection on its promoter, the large-celled PSB *C. okenii*, and the
369 selective metabolic advantage this species gains over other similar microorganisms,
370 namely small-celled PSB and GSB. This was achieved thanks to the possibility of
371 conducting field experiments directly on meromictic Lake Cadagno, where we compared
372 two distinct moments of the year, mid-July, when bioconvection is well present in the BL of
373 the lake, and mid-September, when bioconvection is absent^{30,36}.

374 To the best of our knowledge, to date we lack compelling evidence of how microbes – in
375 natural settings – leverage bioconvection for eco-physiological benefits. A handful of
376 laboratory-based experiments have suggested that microbes put bioconvection to their
377 benefit for exploiting nutritional microenvironments and improved nutrient absorption
378 efficiency^{8,45,46}. For example, experimental observations and fluid dynamic simulations have
379 shown that formation of bioconvection can facilitate oxygen transport, which may in turn
380 benefit aerobic microbial communities, as observed in suspensions of *Bacillus subtilis*⁴⁷.
381 Particularly in natural environments, bioconvection represents an understudied but
382 potentially important mechanism influencing the vertical distribution, and consequently
383 growth and productivity, of the microbial community over different timescales (diurnal and
384 seasonal).

385 Furthermore, bioconvection could play a role in shaping interspecific interactions and mid-
386 to long-term dynamics in the microbial community in meromictic lakes or, for instance,
387 comprise a metabolic competitive advantage for motile species, overcompensating the
388 substantial energy expenditure resulting from swimming against gravity.

389

390 **Chemocline physicochemical parameters**

391 First, we monitored and compared the physico-chemical parameters of Lake Cadagno
392 water column on 16 July and 17 September 2020, which were consistent with past
393 measurements of the same periods^{22,26,38}. The weather trend for Summer 2020 was within
394 the normal range, with good insolation and little precipitation, with the only exception of a
395 heavy thunderstorm in late August that caused a strong mixing of the mixolimnion, and a
396 consequent increase in light penetration to the BL (Storelli *et al.*, manuscript under
397 revision). On 16 July, the water column profile revealed homogeneous temperature and
398 conductivity signatures within the BL, right below the oxic-anoxic interface of the
399 chemocline (Fig. 1c), a proxy of the presence of convective turbulence, which has been
400 shown to be caused by the swimming activity of PSB *C. okenii*^{30, 54}. Therefore, the lack of
401 a uniform layer in the CTD profile of 17 September confirmed the absence of
402 bioconvection in late Summer, further highlighting the seasonality of bioconvection, as
403 already observed in previous studies on Lake Cadagno^{16,53}.

404 Data presented by Sommer *et al.*³⁰ showed how, over the course of three summer
405 seasons (August 2014 and 2015, July 2016), bioconvection activity and thickness of the
406 mixed layer in Lake Cadagno positively correlated with *C. okenii* cell concentration. We
407 refer to the authors' direct numerical simulations (Figure 2 and supporting information
408 Text S3 of the paper) for convincing evidence that the homogeneous layer in Lake
409 Cadagno is due to active biogenic mixing. A detailed explanation of the vertical structure of
410 the mixed layer is provided by Sepúlveda Steiner *et al.*³⁶.

411 Unfortunately, these observations were limited to the time when bioconvection is present.
412 Interestingly, during the period without bioconvection in September, *C. okenii* cell
413 concentration was higher than in July, when bioconvection was well active. This result
414 highlights the complexity of the process driven by the *C. okenii*, seemingly more related to
415 other abiotic or biotic factors investigated in this study, such as light, sulfide or the
416 presence of other phototrophs in the BL, rather than simply to *C. okenii* population size.

417

418 **Light period affects bacterial motility**

419 The importance of photoperiod in shaping bacterial motility has been investigated in
420 several studies. For example, experiments on the flagellated microalga *Chlamydomonas*
421 *reinhardtii*⁴⁸, and other microalgae⁴⁹, revealed that variations in the light-dark period not
422 only markedly affected cell swimming behavior but also influenced cell orientational and
423 gravitactic transport. Similar trends have been presented by other studies on the influence
424 of photoperiod length on the motility rhythm of swimming microorganisms, with important
425 consequences at the population scale^{50–52}.

426 At first the number of cells was identified as a possible factor influencing bioconvection³⁰.
427 However, our results suggest photoperiod is a key factor for the onset of bioconvection. In
428 fact, under the shorter light period of September (12.5 h) no mixed layer is observed within
429 the BL, despite the number of *C. okenii* cells was higher than in July (Fig. 1). Further
430 evidence comes from laboratory experiments, where a reduction in the growth rate of *C.*
431 *okenii* LaCa was observed under a photoperiod of 12/12 h, compared to one of 16/8 h (Di
432 Nezio *et al.*, manuscript in preparation). Interestingly, even after changing light intensity
433 from a chemocline-like value of about 4.0 $\mu\text{mol m}^{-2} \text{s}^{-1}$ PPFD to a 10-fold increase (about
434 40 $\mu\text{mol m}^{-2} \text{s}^{-1}$ PPFD), the reduction in growth was maintained under the 12/12 h
435 photoperiod, further emphasizing the importance of light period rather than its intensity.
436 Bioconvection in Lake Cadagno has also been reported in the absence of light, suggesting
437 the idea of a continued day-night microbial swimming activity independent of phototaxis³⁷.
438 However, it has been suggested that, when nighttime convection occurs, it does so in a
439 fitful fashion and thus only maintaining, rather than expanding, the mixed layer³⁷. The
440 ability of *C. okenii* to swim in a coordinated fashion, even without light attraction, therefore
441 suggests the existence of other biophysical mechanisms coordinating movement.

442

443 **Bioconvection affects sulfide transport across the bacterial layer**

444 The importance of bioconvection in maintaining chemical gradients across the BL,
445 ensuring the constant influx of key elements, has already been proposed in laboratory
446 studies^{35,53}. Interestingly, the higher S^{2-} concentration across the BL observed in July
447 showed that bioconvection transports and homogenizes sulfide from the depths of the lake
448 (Fig. 2 and S3). In addition to carrying more sulfide, an essential requirement for
449 anoxygenic photosynthesis, bioconvection also promotes the removal of oxygen (Fig. 1c,
450 right), which is chemically reduced by S^{2-} . This is further sustained, by higher values of
451 dark CO_2 fixation as observed in September, without bioconvection, than in July (Fig. 4),
452 when sulfide transport reduced oxygen, reiterating the important role of oxygen in the
453 process of chemosynthesis^{28,29,38}.

454 A distinguishing feature of PSB is the production of intracellular sulfur globules (S^0)⁵⁴, that
455 contribute to determining cell internal complexity, correlating with the SSC parameter
456 measured with FCM⁵⁵. On 16 July at sunrise, when bioconvection was active (Fig. 1c),
457 sulfide was detected up to the oxycline, concurrently with a more homogeneous
458 distribution of intracellular complexity between upper and lower BL (Fig. 2). Conversely, at
459 sunrise on 17 September, with no mixed layer, little S^{2-} was detected at the top BL and it
460 mostly remained confined to the lower part, in concomitance with a more pronounced PSB
461 cell granularity at the bottom BL (Fig. 2). Such S^{2-} distribution was likely caused by
462 microbially-generated convective plumes stirring the water also during night, determining a
463 higher concentration of S^{2-} across the whole BL (Fig. 2). Therefore, the distribution of
464 sulfide throughout the BL determines what mean SSC trend in PSB will exhibit. The higher
465 sulfide concentration in the BL during bioconvection was further pointed out by the oxygen
466 profiles (Fig. 1c, right panel). In fact, coinciding with the turbidity peak (>10 FTU) in July,
467 oxygen was consistently absent along the BL, while in September small amounts of
468 scattered oxygen were measured in the upper BL.

469 Given these points, it's clear how bioconvection expand the habitat of the bacterial
470 community, exposing it to light and sweeping S^{2-} along from below.

471

472 **Community dynamics in the bacterial layer**

473 The top-bottom small-celled PSB uniform SSC signal in July correlates well with the
474 hypothesis of *C. okenii* dragging along other microorganisms in the BL, namely small-
475 celled PSB and GSB, that are passively moving floating by means of gas vacuoles^{21,24}. In
476 fact, small-celled PSB and GSB populations distribution across the BL highlighted some
477 interesting patterns (Fig. 3a). Interestingly, while *C. okenii* cells were in general more
478 abundant at the top BL on both times of the season, on 16 July, during active
479 bioconvection, we measured a higher number of small-celled PSB and GSB one meter
480 above the BL than on 17 September (without bioconvection). This finding suggested a
481 negative effect toward other microorganisms competing with *C. okenii* for resources such
482 as sulfide and light. Indeed, bioconvection might push many small-celled PSBs and GSBs
483 out of the optimal BL zone in July (+17%), while this is not observed in September (Fig.
484 3a).

485 The consequences of bioconvection also appear to affect trophic links, such as grazing by
486 zooplankton. A recent study on the predatory activity of the ciliate *Spirostomum teres*,
487 known to feed on PSB⁵⁶, in Lake Cadagno during the years 2020 and 2021 revealed that,
488 in the presence of bioconvection, the amount of *C. okenii* cells ingested by *S. teres* is
489 significantly lower than when bioconvection is absent (Bolick *et al.*, manuscript in
490 preparation).

491 All together, these observations suggest the effective ecological advantage that *C. okenii*
492 has in producing bioconvection.

493

494 **Effect of bioconvection on the primary production**

495 In euxinic environments, light radiation reaching the anaerobic layer is usually positively
496 associated to primary production rates of anaerobic phototrophic sulfur bacteria. The
497 presence of light allows the oxidation of reduced molecules, such as sulfide or sulfur
498 globules, by anaerobic photosynthesis⁵⁷.

499 Our results indicate that photoperiod plays a relevant role in the ability of *C. okenii* to
500 produce bioconvection. Moreover, a different length of the light period can significantly
501 impact photosynthesis itself, by determining higher or lower light-stimulated rates of
502 inorganic carbon uptake as showed in other photosynthetic bacteria^{58–60}, and in PSB and
503 GSB in Lake Cadagno as well. It has been observed that CO₂ fixation in PSB does not
504 occur at a constant rate throughout the day but reaches the highest values in the first
505 hours of light exposure⁶¹, compared with the hours of highest light intensity in the
506 afternoon³⁸. This trend has also been observed in cyanobacteria^{62,63}. For this reason,
507 adopting whole day and night incubations allowed us to avoid underestimate carbon
508 assimilation activity due to diel cycles.

509 In this study, the *in situ* daily ¹⁴C assimilation observed confirmed the strong total inorganic
510 carbon fixation rate in the BL of Lake Cadagno. On 16 July ($6.46 \pm 0.15 \times 10^3$ ¹⁴C amol
511 cell⁻¹ h⁻¹), with 16 h of light, diurnal assimilation was more than three times higher than in
512 September, when values reached only $1.53 \pm 0.04 \times 10^3$ ¹⁴C amol cell⁻¹ h⁻¹ after a
513 daylength of 12.5 h (Fig. 4a). This result is certainly strongly influenced by the
514 physiological activity of *C. okenii*. In fact, its intense fixation activity measured in July was
515 much higher than the other microorganisms analyzed (Fig. 4). The situation changed
516 radically in September, when in the absence of bioconvection, *C. okenii* loses dominance
517 over inorganic carbon fixation in favor of the small-celled PSB *T. syntrophicum* Cad16^T.
518 These findings, in combination with the increase in numbers shown by FISH for all species
519 of small-celled PSB (Fig. 3b), further indicate that bioconvection exerts a negative
520 influence on other microorganisms competing for the same resources as *C. okenii*.

521 Similarly, the higher dark ^{14}C assimilation rates observed in July in the BL and in *C. okenii*
522 pure culture (Fig. 4a,b) suggests the persistence of bioconvection during nighttime in Lake
523 Cadagno³⁷. In addition, quantum requirements of CO_2 fixation for each of the three species
524 incubated with carbon-14 were calculated as moles of photons required to assimilate a
525 mole of $^{14}\text{CO}_2$. The value obtained for *C. okenii* in July (10.6) was similar to that reported
526 by Brune⁴¹, who calculated quantum requirements of 8.5 - 10.5 quanta per CO_2 fixed for
527 PSB and 3.3 - 4.5 for GSB, under optimum laboratory conditions, while *T. syntrophicum*
528 and *C. phaeobacteroides* had much higher requirements (23.4 and 74.9, respectively).
529 Under the September light regime, *C. okenii* performed significantly worse (38.5), while *T.*
530 *syntrophicum* (13.5) and *C. phaeobacteroides* (39.1) had both lower quantum
531 requirements than in July. Applying what observed in the ^{14}C -incubated cultures to the
532 broader environmental context of the lake, our data provide enough evidence to sustain
533 that light regime played a key role, as it provided *C. okenii* cells with the energy required
534 for the onset of bioconvection.

535

536 **Transcriptomic reveals different gene expression levels**

537 In September the cellular activity of *C. okenii* was much higher compared to July, with the
538 presence of various transcribed genes. The upregulation in *C. okenii* of anoxygenic
539 photosynthesis-related genes in September (Tab. S1) suggests a compensation
540 mechanism for a less efficient photosynthetic activity in the absence of bioconvection and
541 under less favorable light conditions^{64,65}. Data from transcriptomic analyses on *C. okenii*
542 corroborated these findings showing higher expression levels of genes involved in the
543 photoautotrophic sulfur oxidation when in absence of bioconvection.
544 However, despite the significant contributions transcriptomics has made to the field of
545 microbial ecology, some limitations have emerged in the application of this techniques to
546 the study of physiological responses to the environment⁶⁶. The main constraints are

547 related to the fact that genes with relevant impact on fitness are rare and therefore difficult
548 to detect by transcript analysis, and besides, the relationship between gene expression
549 and fitness is often dubious. Another limit is that fitness is mostly determined by protein
550 activity and the amount of mRNA is a poor indicator of the amount of protein⁶⁷.
551 Nonetheless, (meta)transcriptomics has the potential of providing valuable insights into
552 environmental microbial communities.

553

554 **Conclusions**

555 In this paper, we combined biological, chemical and physical factors to elucidate how
556 bioconvection shape the main eco-physiological traits for the phototrophic sulfur bacteria
557 community inhabiting the BL of Lake Cadagno. We first report the key role of the
558 photoperiod length by comparing two different period of measurements. Moreover, we
559 showed how the presence of bioconvection contributes to maintaining a sulfide gradient
560 across the BL, thereby promoting oxygen removal and avoiding consumption of
561 intracellular storage substances such as sulfur globules, requiring a greater energy
562 investment (also shown by the high transcriptional activity in the absence of
563 bioconvection). It is also interesting to note that bioconvection negatively affects the fitness
564 of the other ecological competitors of *C. okenii*, namely small-celled PSB and GSB,
565 present in the BL. Overall, our combined data suggest that *C. okenii* is able to gain a
566 competitive advantage over other non-motile phototrophic sulfur bacteria in the quest for
567 the optimal environmental conditions by producing mixed layers through bioconvection.
568
569 Nevertheless, despite this study provides evidence of the eco-physiological effects of
570 bioconvection in an environmental setting, its consequences on the microenvironmental
571 conditions and the other (micro)organisms involved need to be substantiated with further
572 studies. In particular, the role of bioconvection on the transport of sulfide across the BL,

573 and further insights on its production by sulfate-reducing bacteria in the monimolimnion,
574 require a more detailed investigation. Impacts of bioconvection might also extend outside
575 the mixed layer, influencing the interaction between phototrophic sulfur bacteria and the
576 zooplankton living just above the bacterial layer, e.g., in terms of predation and/or
577 distribution patterns. Lastly, a deeper understanding of the motility mechanisms of *C.*
578 *okenii* triggering bioconvection at the single-cell level will help unravelling the nature of this
579 multi-scale process.
580

581

582 **References**

- 583 1. Ochiai, N., Draglila, M. I. & Parke, J. L. Pattern swimming of *Phytophthora citricola*
584 zoospores: An example of microbial bioconvection. *Fungal Biol.* **115**, 228–235 (2011).
- 585 2. Abe, T., Nakamura, S. & Kudo, S. Bioconvection induced by bacterial chemotaxis in a
586 capillary assay. *Biochem. Biophys. Res. Commun.* **483**, 277–282 (2017).
- 587 3. Ghorai, S. & Panda, M. K. Bioconvection in an anisotropic scattering suspension of
588 phototactic algae. *Eur. J. Mech. - B/Fluids* **41**, 81–93 (2013).
- 589 4. Hill, N. A. & Pedley, T. J. Bioconvection. *Fluid Dyn. Res.* **37**, 1–20 (2005).
- 590 5. Yanaoka, H. & Nishimura, T. Pattern wavelengths and transport characteristics in three-
591 dimensional bioconvection generated by chemotactic bacteria. *J. Fluid Mech.* **952**, (2022).
- 592 6. Bouffard, D. & Wüest, A. Convection in Lakes. *Annu. Rev. Fluid Mech.* **51**, 189–215 (2019).
- 593 7. Bees, M. A. Advances in Bioconvection. *Annu. Rev. Fluid Mech.* **2020** **52**, 449–476 (2020).
- 594 8. Sengupta, A. Planktonic Active Matter. (2023)
595 doi:<https://doi.org/10.48550/arXiv.2301.09550>.
- 596 9. Andrei, A. Ş. *et al.* Contrasting taxonomic stratification of microbial communities in two
597 hypersaline meromictic lakes. *ISME J.* **2015** **9**, 2642–2656 (2015).
- 598 10. Block, K. R., O'Brien, J. M., Edwards, W. J. & Marnocha, C. L. Vertical structure of the
599 bacterial diversity in meromictic Fayetteville Green Lake. *Microbiologyopen* **10**, e1228
600 (2021).
- 601 11. Gulati, R., Zadereev, E. & Degermendzhi, A. Ecology of Meromictic Lakes. in (eds. Gulati,
602 R. D., Zadereev, E. S. & Degermendzhi, A. G.) 398 (Springer International Publishing,
603 2017).
- 604 12. Tonolla, M. *et al.* Lake Cadagno: Microbial Life in Crenogenic Meromixis. in *Ecology of*
605 *Meromictic Lakes* (eds. Gulati, R., Zadereev, E. & Degermendzhi, A.) 155–186 (Springer
606 International Publishing, 2017). doi:10.1007/978-3-319-49143-1_7.
- 607 13. Rogozin, D. Y., Trusova, M. Y., Khromechek, E. B. & Degermendzhy, A. G. Microbial
608 community of the chemocline of the meromictic Lake Shunet (Khakassia, Russia) during

- 609 summer stratification. *Microbiology* **79**, 253–261 (2010).
- 610 14. Del Don, C., Hanselmann, K. W., Peduzzi, R. & Bachofen, R. The meromictic alpine Lake
611 Cadagno: Orographical and biogeochemical description. *Aquat. Sci.* **63**, 70–90 (2001).
- 612 15. Tonolla, M. *et al.* Lake Cadagno: Microbial Life in Crenogenic Meromixis. in *Ecology of*
613 *Meromictic Lakes* (eds. Gulati, R., Zadereev, E. S. & Degermendzhi, A.) vol. 228 155–186
614 (Springer International Publishing, 2017).
- 615 16. Danza, F. *et al.* Bacterial diversity in the water column of meromictic Lake Cadagno and
616 evidence for seasonal dynamics. *PLoS One* **13**, 1–17 (2018).
- 617 17. Decristophoris, P. M. A., Peduzzi, S., Ruggeri-Bernardi, N., Hahn, D. & Tonolla, M. Fine
618 scale analysis of shifts in bacterial community structure in the chemocline of meromictic
619 Lake Cadagno, Switzerland. *J. Limnol.* **68**, 16–24 (2009).
- 620 18. Ravasi, D. F. *et al.* Development of a real-time PCR method for the detection of fossil 16S
621 rDNA fragments of phototrophic sulfur bacteria in the sediments of Lake Cadagno. 196–204
622 (2012) doi:10.1111/j.1472-4669.2012.00326.x.
- 623 19. Tonolla, M., Peduzzi, R. & Hahn, D. Long-Term Population Dynamics of Phototrophic Sulfur
624 Bacteria in the Chemocline of Lake Cadagno, Switzerland. *Appl. Environ. Microbiol.* **71**,
625 3544–3550 (2005).
- 626 20. Saini, J. S. *et al.* Bacterial, Phytoplankton, and Viral Distributions and Their Biogeochemical
627 Contexts in Meromictic Lake Cadagno Offer Insights into the Proterozoic Ocean Microbial
628 Loop. *MBio* **13**, (2022).
- 629 21. Luedin, S. M. *et al.* Complete genome sequence of ‘Thiodictyon syntrophicum’ sp. nov.
630 strain Cad16 T , a photolithoautotrophic purple sulfur bacterium isolated from the alpine
631 meromictic Lake Cadagno. *Stand. Genomic Sci.* **13**, 1–13 (2018).
- 632 22. Luedin, S. M. *et al.* Draft Genome Sequence of Chromatium okenii Isolated from the
633 Stratified Alpine Lake Cadagno. *Sci. Rep.* **9**, 1–14 (2019).
- 634 23. Peduzzi, S. *et al.* Thiocystis chemoclinalis sp. nov. and thiocystis cadagnonensis sp. nov.,
635 motile purple sulfur bacteria isolated from the chemocline of a meromictic lake. *Int. J. Syst.*
636 *Evol. Microbiol.* **61**, 1682–1687 (2011).

- 637 24. Peduzzi, S. *et al.* Candidatus ‘Thiodictyon syntrophicum’, sp. nov., a new purple sulfur
638 bacterium isolated from the chemocline of Lake Cadagno forming aggregates and specific
639 associations with *Desulfocapsa* sp. *Syst. Appl. Microbiol.* **35**, 139–144 (2012).
- 640 25. Posth, N. R. *et al.* Carbon isotope fractionation by anoxygenic phototrophic bacteria in
641 euxinic Lake Cadagno. *Geobiology* **15**, 798–816 (2017).
- 642 26. Danza, F., Storelli, N., Roman, S., Lüdin, S. & Tonolla, M. Dynamic cellular complexity of
643 anoxygenic phototrophic sulfur bacteria in the chemocline of meromictic Lake Cadagno.
644 *PLoS One* **12**, 1–17 (2017).
- 645 27. Philippi, M. *et al.* Purple sulfur bacteria fix N₂ via molybdenumnitrogenase in a low
646 molybdenum Proterozoic ocean analogue. *Nat. Commun.* 1–12 doi:10.1038/s41467-021-
647 25000-z.
- 648 28. Berg, J. S. *et al.* Dark aerobic sulfide oxidation by anoxygenic phototrophs in anoxic waters.
649 *Environ. Microbiol.* (2019) doi:10.1111/1462-2920.14543.
- 650 29. Luedin, S. M. *et al.* Mixotrophic growth under micro-oxic conditions in the purple sulfur
651 bacterium “thiodictyon syntrophicum”. *Front. Microbiol.* **10**, 1–15 (2019).
- 652 30. Sommer, T. *et al.* Bacteria-induced mixing in natural waters. *Geophys. Res. Lett.* **44**, 9424–
653 9432 (2017).
- 654 31. Sato, N., Sato, K. & Toyoshima, M. Analysis and modeling of the inverted bioconvection in
655 *Chlamydomonas reinhardtii*: emergence of plumes from the layer of accumulated cells.
656 *Heliyon* **4**, e00586 (2018).
- 657 32. Kunze, E., Dower, J. F., Bevaridge, I., Bawey, R. & Bartlett, K. P. Observations of
658 Biologically Generated Turbulence in a Coastal Inlet. *Science (80-.)*. **313**, 1768–1770
659 (2006).
- 660 33. Kils, U. FORMATION OF MICROPATCHES BY ZOOPLANKTON-DRIVEN
661 MICROTURBULENCES. *Bull. Mar. Sci.* **53**, 160–169 (1993).
- 662 34. Widdel, F. *et al.* Ferrous Iron Oxidation by Anoxygenic Phototrophic Bacteria. *Nature* **362**,
663 834–836 (1993).
- 664 35. Bearon, R. N. & Grünbaum, D. Bioconvection in a stratified environment: Experiments and

- 665 theory. *Phys. Fluids* **18**, (2006).
- 666 36. Sepúlveda Steiner, O., Bouffard, D. & Wüest, A. Convection-diffusion competition within
667 mixed layers of stratified natural waters. *Geophys. Res. Lett.* **46**, 1–10 (2019).
- 668 37. Sepúlveda Steiner, O. R., Damien Bouffard & Wüest, A. Persistence of bioconvection-
669 induced mixed layers in a stratified lake. *Limnol. Oceanogr.* 1–17 (2021).
- 670 38. Di Nezio, F. *et al.* Anoxygenic photo- and chemo-synthesis of phototrophic sulfur bacteria
671 from an alpine meromictic lake. *FEMS Microbiol. Ecol.* **97**, 1–17 (2021).
- 672 39. Eichler, B. & Pfennig, N. A new purple sulfur bacterium from stratified freshwater lakes,
673 *Amoebobacter purpureus* sp. nov. *Arch. Microbiol.* **149**, 395–400 (1988).
- 674 40. Gächter, R., Marès, A., Gächter, R. & Mares, A. Comments to the Acidification and Bubbling
675 Method for Determining Phytoplankton Production. *Oikos* **33**, 69 (1979).
- 676 41. Brune, D. C. Sulfur oxidation by phototrophic bacteria. *Biochim. Biophys. Acta* **975**, 189–221
677 (1989).
- 678 42. Love, M. I., Soneson, C., Patro, R., Vitting-Seerup, K. & Thodberg, M. Swimming
679 downstream: statistical analysis of differential transcript usage following Salmon
680 quantification. *F1000Research* 2018 7952 **7**, 952 (2018).
- 681 43. Mölder, F. *et al.* Sustainable data analysis with Snakemake. *F1000Research* 2021 1033 **10**,
682 33 (2021).
- 683 44. Dahl, C. & Prange, A. Bacterial Sulfur Globules: Occurrence, Structure and Metabolism. in
684 *Inclusions in Prokaryotes* (ed. Shively, J. M.) 21–51 (Springer Berlin Heidelberg, 2006).
685 doi:10.1007/7171.
- 686 45. Shoup, D. & Ursell, T. Bacterial bioconvection confers context-dependent growth benefits
687 and is robust under varying metabolic and genetic conditions. *bioRxiv* 2021.04.20.440374
688 (2021) doi:10.1101/2021.04.20.440374.
- 689 46. Ni, B., Colin, R., Link, H., Endres, R. G. & Sourjik, V. Growth-rate dependent resource
690 investment in bacterial motile behavior quantitatively follows potential benefit of chemotaxis.
691 *Proc. Natl. Acad. Sci. U. S. A.* **117**, 595–601 (2020).
- 692 47. Tuval, I. *et al.* Bacterial swimming and oxygen transport near contact lines. *Proc. Natl. Acad.*

- 693 *Sci. U. S. A.* **102**, 2277–2282 (2005).
- 694 48. Jin, D., Kotar, J., Silvester, E., Leptos, K. C. & Croze, O. A. Diurnal Variations in the Motility
695 of Populations of Biflagellate Microalgae. *Biophys. J.* **119**, 2055–2062 (2020).
- 696 49. Richter, P. R. *et al.* Influence of Different Light-Dark Cycles on Motility and Photosynthesis
697 of *Euglena gracilis* in Closed Bioreactors. *Astrobiology* **14**, 848 (2014).
- 698 50. Lerch, K. A. & Cook, C. B. Some Effects of Photoperiod on the Motility Rhythm of Cultured
699 Zooxanthellae. *Bull. Mar. Sci.* **34**, 477–483 (1984).
- 700 51. Fitt, W. K. & Trench, R. K. The Relation of Diel Patterns of Cell Division to Diel Patterns of
701 Motility in the Symbiotic Dinoflagellate *Symbiodinium microadriaticum* Freudenthal in
702 Culture. *New Phytol.* **94**, 421–432 (1983).
- 703 52. Barnett, A., Méléder, V., Dupuy, C. & Lavaud, J. The Vertical Migratory Rhythm of Intertidal
704 Microphytobenthos in Sediment Depends on the Light Photoperiod, Intensity, and Spectrum:
705 Evidence for a Positive Effect of Blue Wavelengths. *Front. Mar. Sci.* **7**, 212 (2020).
- 706 53. Findlay, A. J., Di Toro, D. M. & Luther, G. W. A model of phototrophic sulfide oxidation in a
707 stratified estuary. *Limnol. Oceanogr.* **62**, 1853–1867 (2017).
- 708 54. Frigaard, N. U. & Dahl, C. Sulfur Metabolism in Phototrophic Sulfur Bacteria. *Adv. Microb.*
709 *Physiol.* **54**, 103–200 (2008).
- 710 55. Danza, F. Flow cytometry as a tool to investigate the anoxygenic phototrophic sulfur
711 bacteria coexistence in the chemocline of meromictic Lake Cadagno. (Université de
712 Genève, 2018).
- 713 56. Bolick, L. 'A microbial whale' - the giant ciliate *Spirostomum teres* feeding on phototrophic
714 sulfur bacteria in Lake Cadagno (Ticino). (University of Zürich, 2022).
- 715 57. Parkin, T. B. & Brock, T. D. Photosynthetic bacterial production in lakes: The effects of light
716 intensity. *Limnol. Oceanogr.* **25**, 711–718 (1980).
- 717 58. Xu, K., Zou, X., Xue, Y., Qu, Y. & Li, Y. The impact of seasonal variations about temperature
718 and photoperiod on the treatment of municipal wastewater by algae-bacteria system in lab-
719 scale. *Algal Res.* **54**, 102175 (2021).
- 720 59. Zhou, Q., Zhang, P., Zhang, G. & Peng, M. Biomass and pigments production in

- 721 photosynthetic bacteria wastewater treatment: Effects of photoperiod. *Bioresour. Technol.*
722 **190**, 196–200 (2015).
- 723 60. Gunawan, T. J., Ikhwan, Y., Restuhadi, F. & Pato, U. Effect of light Intensity and
724 photoperiod on growth of *Chlorella pyrenoidosa* and CO₂ Biofixation. *E3S Web Conf.* **31**,
725 03003 (2018).
- 726 61. Storelli, N. *et al.* CO₂ assimilation in the chemocline of Lake Cadagno is dominated by a few
727 types of phototrophic purple sulfur bacteria. *FEMS Microbiol. Ecol.* **84**, 421–432 (2013).
- 728 62. Paul, J. H., Kang, J. B. & Tabita, F. R. Diel patterns of regulation of *rbcl* transcription in a
729 cyanobacterium and a prymnesiophyte. *Mar. Biotechnol.* **2**, 429–436 (2000).
- 730 63. Wyman, M. Diel rhythms in ribulose-1,5-bisphosphate carboxylase/oxygenase and
731 glutamine synthetase gene expression in a natural population of marine picoplanktonic
732 cyanobacteria (*Synechococcus* spp.). *Appl. Environ. Microbiol.* **65**, 3651–3659 (1999).
- 733 64. Fischer, C., Wiggli, M., Schanz, F., Hanselmann, K. W. & Bachofen, R. Light environment
734 and synthesis of bacteriochlorophyll by populations of *Chromatium okenii* under natural
735 environmental conditions. *FEMS Microbiol. Ecol.* **21**, 1–9 (1996).
- 736 65. Serdyuk, O. P., Smolygina, L. D. & Ashikhmin, A. A. A New Type of Light-Harvesting
737 Complex Detected when Growing *Rhodospseudomonas palustris* under Low Light Intensity
738 Conditions. *Dokl. Biochem. Biophys.* **491**, 101–104 (2020).
- 739 66. Evans, T. G., Podrabsky, J. E., Stillman, J. H. & Tomanek, L. Considerations for the use of
740 transcriptomics in identifying the ‘genes that matter’ for environmental adaptation. *J. Exp.*
741 *Biol.* **218**, 1925–1935 (2015).
- 742 67. Aguiar-Pulido, V. *et al.* Metagenomics, Metatranscriptomics, and Metabolomics Approaches
743 for Microbiome Analysis. *Evol. Bioinform. Online* **12**, 5 (2016).

744

745 **Acknowledgments**

746 We thank G. Ranieri and M. Thelen for technical assistance with ¹⁴C experiment analyses;
747 M. Tonolla and F. Danza for fruitful discussion and constructive comments on the
748 manuscript; the Alpine Biology Centre Foundation (CBA) for laboratory facilities and

749 housing. Funding was provided by the Swiss National Science Foundation (grant number
750 315230-179264) and by the Institute of Microbiology (IM) of the University of Applied
751 Sciences and Arts of Southern Switzerland (SUPSI). A. Sengupta thanks the ATTRACT
752 Investigator Grant (No. A17/MS/11572821/MBRACE) and FNR-CORE Grant (No.
753 C19/MS/13719464/TOPOFLUME/Sengupta) from the Luxembourg National Research
754 Fund for supporting this work.

755

756 **Author contributions**

757 FDN, SR, ABD, and NS designed research; FDN, SR, ABD, and NS collected samples;
758 FDN and SR performed laboratory work; FDN, SR, OSS and ABD analyzed data; FDN
759 and NS wrote the paper. All authors developed the concepts and hypotheses covered in
760 this work, and have contributed to the revisions of the manuscript.

761

762 **Competing interests**

763 The authors declare that no competing interests exist.